STRUCTURAL BIOLOGY COMMUNICATIONS

ISSN 2053-230X

# Preparation of stable recombinant Osm1 noncovalently bound with flavin adenosine dinucleotide cofactor for structural study

Sunghwan Kim[a,b]* and Hyun Ho Park[c]*

[a]New Drug Development Center, Daegu-Gyeongbuk Medical Innovation Foundation, Daegu, Republic of Korea, [b]R&D Center, Polus Inc., 32 Songdogwahak-ro, Yeonsu-gu, Incheon, Republic of Korea, and [c]College of Pharmacy, Chung-Ang University, 84 Heukseok-ro, Dongjak-gu, Seoul 06974, Republic of Korea. *Correspondence e-mail: sunghwan.kim@polus-global.com, hyunho@ynu.ac.kr

Received 2 October 2018
Accepted 4 January 2019

Edited by M. J. Romao, Universidade Nova de Lisboa, Portugal

**Keywords:** soluble fumarate reductase; anaerobiosis; Osm1; limited proteolysis; stabilization; crystallization.

Osm1, a soluble fumarate reductase from *Saccharomyces cerevisiae*, is localized in both the mitochondria and the endoplasmic reticulum (ER). *OSM1* genetically interacts with *ERO1*, which encodes an essential ER oxidoreductase for disulfide-bond formation under anaerobic conditions. However, the detailed enzymatic mechanisms involved in this interaction and the cellular roles of Osm1 are not fully understood. In this study, monomeric and stable recombinant Osm1 was successfully prepared for structural study. During purification, it was realized that the majority of recombinant Osm1 expressed in *Escherichia coli* lacked the flavin adenosine dinucleotide (FAD) cofactor. However, exogenously introduced FAD could be incorporated into recombinant Osm1, generating stable and homogenous holo Osm1. Moreover, after removing a flexible fragment by limited proteolysis, holo Osm1 formed isotropic crystals that retained catalytic activity. X-ray diffraction data were successfully collected from the Osm1 crystals to a resolution of 1.75 Å.

## 1. Introduction

Fumarate reductase reduces fumarate to succinate by transferring electrons from the cofactor flavin adenosine dinucleotide (FAD) to fumarate under anaerobic conditions (Reid *et al.*, 2000). Fumarate reductases are categorized as membrane-bound or soluble (Miura *et al.*, 2008). While membrane-bound fumarate reductases contain covalently bound FAD that mediates bidirectional enzyme reactions, soluble fumarate reductases contain noncovalently bound FAD that mediates a unidirectional enzyme reaction. In bacteria, membrane-bound fumarate reductases play critical roles as terminal oxidants for anaerobic respiration-mediated ATP synthesis (Cecchini *et al.*, 2002). Some bacteria contain soluble fumarate reductases, such as flavocytochrome $c_3$ fumarate reductase ($Fcc_3$) produced by *Shewanella* sp. (Bamford *et al.*, 1999; Pealing *et al.*, 1992).

In *Saccharomyces cerevisiae*, two soluble fumarate reductases are encoded by the *FRDS* and *OSM1* genes, which are critical for anaerobiosis (Arikawa *et al.*, 1998). Simultaneous disruption of the *FRDS* and *OSM1* genes results in an inability of this organism to grow anaerobically on glucose as a carbon source, and disruption of the *OSM1* gene causes poor growth under anaerobic conditions (Enomoto *et al.*, 2002; Arikawa *et al.*, 1998). Frd1, the product of the *FRDS* gene, is localized in the cytosol, while Osm1, the product of the *OSM1* gene, has been reported to be a promitochondrial protein (Arikawa *et al.*, 1998; Muratsubaki & Enomoto, 1998). However, a recent study showed that Osm1 localizes in both the endoplasmic

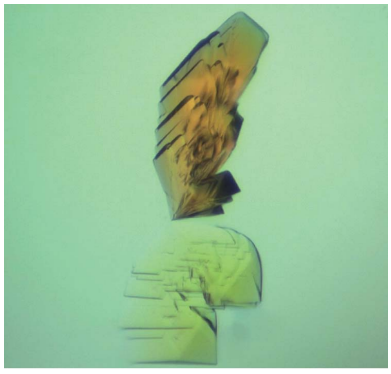

reticulum (ER) and the mitochondria depending on two different start codons, Met1 and Met33 (Williams *et al.*, 2014). Sequence analysis also predicted that Osm1 contains a signal sequence for ER localization (Williams *et al.*, 2014) and that the N-glycoproteome includes Osm1 (Zielinska *et al.*, 2012), supporting ER localization of Osm1. Considering the functions of the ER, ER-resident soluble fumarate reductase must have distinct roles from bacterial soluble fumarate reductase, which is involved in anaerobic respiration. In support of this assumption, *S. cerevisiae* does not utilize anaerobic respiration for ATP synthesis under anaerobic conditions and instead employs fermentation, which does not necessitate fumarate reduction. Osm1 and Frd1 appear to play roles in redox balancing and protein production during anaerobiosis (Bergdahl *et al.*, 2014; Enomoto *et al.*, 2002; Liu *et al.*, 2013).

Despite recent efforts to understand the process by which Osm1 functions and its important emerging role in both the ER and mitochondria, no structural information is currently available. Therefore, in this study, we overexpressed and purified recombinant Osm1 to enable a structural and biochemical study of Osm1 in order to elucidate its molecular mechanism. During the purification step, we realized that the majority of recombinant Osm1 lacked the flavin adenosine dinucleotide (FAD) cofactor and therefore exhibited less stable and heterogeneous conformations. However, we were able to overcome this problem by incorporating FAD cofactor into purified recombinant Osm1, which resulted in monomeric, homogenous and stable holo Osm1. Moreover, removal of the flexible terminus of Osm1 by limited proteolysis enabled the generation of crystals that provided high-quality diffraction data.

## 2. Materials and methods

### 2.1. Macromolecule production

Osm1 DNA corresponding to residues Met33–Tyr501 was inserted into the pET-28a vector using the NheI and XhoI restriction sites, resulting in an N-terminal fusion to a 6×His tag and a thrombin cleavage site. Cloned plasmid DNA was transformed into *Escherichia coli* BL21 (DE3) competent cells (New England Biolabs). The transformed cells were cultured in lysogeny broth (LB) and expression of Osm1 was induced with 80 µg ml$^{-1}$ isopropyl $\beta$-D-1-thiogalactopyranoside (IPTG) for 20 h at 293 K. The cells were then harvested by centrifugation and sonicated in resuspension buffer (20 m*M* sodium phosphate pH 7.4, 500 m*M* NaCl, 25 m*M* imidazole and protease-inhibitor cocktail). The cell lysates were then clarified by centrifugation at 27 000*g* for 1 h, which was followed by filtration using a 0.22 µm filter. Clarified samples were loaded onto a 5 ml HiTrap column (GE Healthcare Life Science) and eluted using a 25–500 m*M* imidazole gradient after adequate washing with resuspension buffer. Nickel-purified Osm1 was further purified by size-exclusion chromatography on a Superdex 200 Increase 10/300 GL column (GE Healthcare Life Science) with 25 m*M* sodium phosphate pH 7.4, 150 m*M* NaCl, 1 m*M* EDTA. Purification steps were monitored by SDS–PAGE analysis. Macromolecule-production information is given in Table 1.

**Table 1**
Macromolecule-production information.

| | |
|---|---|
| Source organism | Yeast (*Saccharomyces cerevisiae*) |
| DNA source | *S. cerevisiae* genomic DNA (GenBank CAA89579) |
| Forward primer | AGTCTTGCTAGCATGAAACAACCAGTGGTG GTC |
| Reverse primer | GTGGTGCTCGAGCTAGTACAATTTTGCTAT GTTATCC |
| Cloning vector | pET-28a |
| Expression vector | pET-28a |
| Expression host | *E. coli* |
| Complete amino-acid sequence of the construct produced | MGSSHHHHHHSSGLVPRGSSMKQPVVVIGS GLAGLTTSNRLISKYRIPVVLLDKAASI GGNSIKASSGINGAHTDTQQNLKVMDTP ELFLKDTLHSAKGRGVPSLMDKLTKESK SAIRWLQTEFDLKLDLLAQLGGHSVPRT HRSSGKLPPGFEIVQALSKKLKDISSKD SNLVQIMLNSEVVDIELDNQGHVTGVVY MDENGNRKIMKSHHVVFCSGGFGYSKEM LKEYSPNLIHLPTTNGKQTTGDGQKILS KLGAELIDMDQVQVHPTGFIDPNDRENN WKFLAAEALRGLGGILLHPTTGRRFTNE LSTRDTVTMEIQSKCPKNDNRALLVMSD KVYENYTNNINFYMSKNLIKKVSINDLI RQYDLQTTASELVTELKSYSDVNTKDTF DRPLIINAFDKDISTESTVYVGEVTPVV HFTMGGVKINEKSQVIKKNSESVLSNGI FAAGEVSGGVHGANRLGGSSLLECVVFG KTAADNIAKLY |

### 2.2. FAD-binding analysis

To determine the occupancy of FAD in recombinant Osm1, purified Osm1 was denatured with 6 *M* guanidine–HCl to release the FAD. The protein concentration was then determined using the Bradford protein assay (Bio-Rad), comparing the results with a standard curve for bovine serum albumin (BSA). The FAD concentration was determined by measuring the fluorescence with excitation and emission at 450 and 535 nm, respectively, and comparing the results with a standard curve for free FAD in 6 *M* guanidine–HCl. The FAD stock concentration was measured based on $A_{450}$ (absorbance at 450 nm) and an extinction coefficient of 11 300 $M^{-1}$ cm$^{-1}$. To obtain the holoenzyme, purified Osm1 at 10 µ*M* was incubated with 100 µ*M* FAD for 1 h on ice. Unbound free FAD was removed by passing the sample through a Zeba Spin Desalting Column (ThermoFisher Scientific). The protein concentration and the protein-bound FAD concentration of holo Osm1 were also determined as described above.

Changes in the response to the addition of FAD were monitored by native (nondenaturing) PAGE using a PhastSystem (GE Healthcare) with pre-made 8–25% acrylamide gradient gels (GE Healthcare). Purified recombinant Osm1 was incubated with 10 m*M* fumarate or 100 µ*M* FAD at room temperature for 1 h before loading the gel. Coomassie Brilliant Blue was used to stain and detect shifted bands. The stability of Osm1 was determined by measuring melting curves using Protein Thermal Shift dye (Invitrogen) in a StepOnePlus Real-Time PCR System (ThermoFisher Scientific) according to the manufacturer's instructions. Briefly, 2 µg Osm1 was

mixed with 1× Protein Thermal Shift dye and buffer in a 20 µl volume and the changes in signal upon protein denaturation were monitored as the temperature increased from 40 to 80°C.

### 2.3. Limited proteolysis

To remove flexible terminal fragments, purified Osm1 was treated with different amounts of trypsin (Promega) at weight ratios of 1:1000 to 1:20 (Osm1:trypsin). Trypsinized Osm1 was analyzed by reducing SDS–PAGE. For large-scale limited proteolysis, 10 mg purified Osm1 was treated with 20 µg

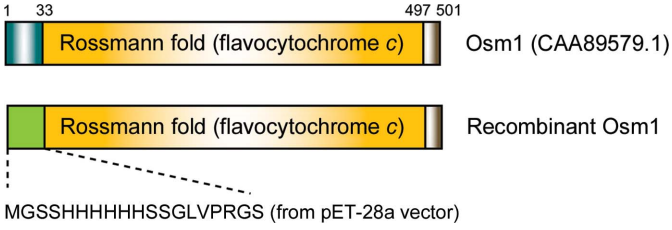


**Figure 1**
The Osm1 construct for *E. coli* expression. Osm1 from *S. cerevisiae* is predicted to have a Rossmann fold similar to that in flavocytochrome *c*. The DNA sequence for Osm1 (residues Met33–Tyr501) was inserted into the pET-28a vector, with a 6×His tag and a thrombin cleavage site at the N-terminus.

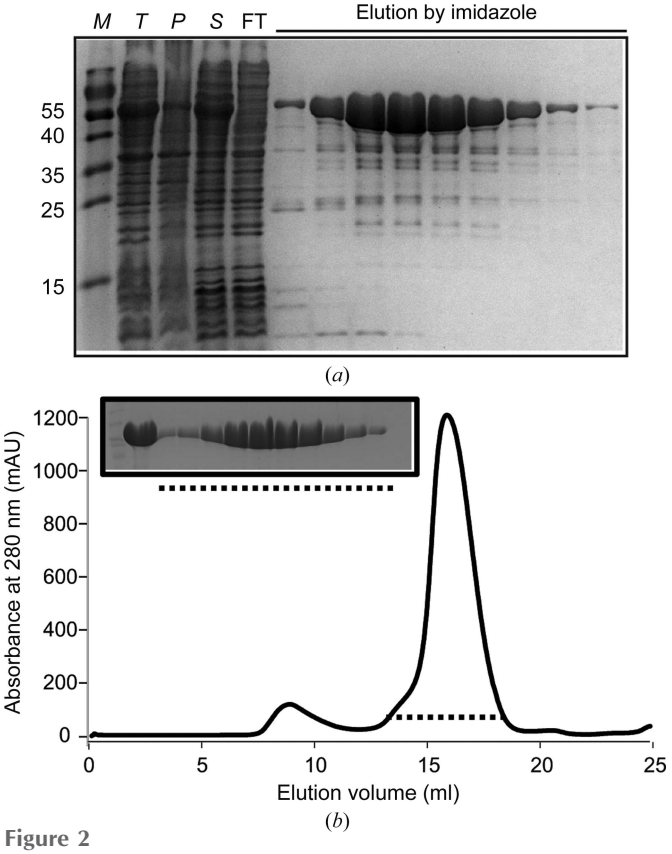


**Figure 2**
Purification of recombinant Osm1. (*a*) Osm1 was purified by NTA-affinity chromatography and analysed by SDS–PAGE. Lane *M*, molecular-mass markers (labelled in kDa); lane *T*, total lysate; lane *P*, pellet; lane *S*, soluble fraction; lane FT, flowthrough. (*b*) Osm1 was further purified by size-exclusion chromatography. The inset shows an SDS–PAGE analysis of the elution fractions indicated by the dashed line.

**Table 2**
Crystallization.

| | |
|---|---|
| Method | Hanging-drop vapour diffusion |
| Plate type | 24-well plates from Hampton Research |
| Temperature (K) | 293 |
| Protein concentration (mg ml$^{-1}$) | 10 |
| Buffer composition of protein solution | 20 m*M* Tris pH 7.4, 150 m*M* NaCl, 2 m*M* TCEP, 200 µ*M* FAD, 5 m*M* fumarate |
| Composition of reservoir solution | 25%(*w*/*v*) PEG 3500, 0.2 *M* NaCl, 0.1 *M* bis-Tris pH 5.5 |
| Volume and ratio of drop | 200 nl, 1:1 |
| Volume of reservoir (µl) | 100 |

**Table 3**
Data collection and processing.

Values in parentheses are for the outer shell.

| | |
|---|---|
| Diffraction source | 5C SBII, PAL |
| Wavelength (Å) | 0.97760 |
| Temperature (K) | 110 |
| Detector | ADSC Quantum 315r |
| Crystal-to-detector distance (mm) | 250 |
| Rotation range per image (°) | 1 |
| Total rotation range (°) | 360 |
| Exposure time per image (s) | 1 |
| Space group | $P2_1$ |
| *a*, *b*, *c* (Å) | 43.88, 109.32, 49.93 |
| α, β, γ (°) | 90.00, 112.25, 90.00 |
| Mosaicity (°) | 0.3 |
| Resolution range (Å) | 50–1.75 |
| Perfect twinning test† | 1.95 |
| Total No. of reflections | 164160 |
| No. of unique reflections | 41426 |
| Completeness (%) | 94.5 (100) |
| Multiplicity | 4.0 (4.2) |
| $\langle I/\sigma(I)\rangle$ | 33.1 (6.5) |
| $R_{\rm r.i.m.}$ | 3.5 (16.3) |
| $CC_{1/2}$ (%) | 99.1 (93.1) |

† The perfect twinning test calculates $\langle I^2\rangle/\langle I\rangle^2$, which has values of 2.0 for an untwinned crystal and 1.5 for a perfectly twinned crystal.

trypsin in Tris-based saline containing 2 m*M* $CaCl_2$, after which the reaction was quenched with 10 µ*M* leupeptin (Sigma). Trypsin-resistant Osm1 was loaded onto a Mono S column (GE Healthcare Life Science) and eluted with a linear gradient of salt by mixing buffer *A* (20 m*M* MES pH 6.5, 1 m*M* EDTA) and buffer *B* (1.5 *M* NaCl, 20 m*M* MES pH 6.5, 1 m*M* EDTA). Purified trypsin-resistant Osm1 was concentrated to 10 mg ml$^{-1}$ in 20 m*M* Tris pH 7.4, 150 m*M* NaCl, 2 m*M* Tris(2-carboxyethyl)phosphine (TCEP), 200 µ*M* FAD (Sigma), 5 m*M* fumarate (Sigma) for crystallization.

### 2.4. Catalytic activity assay

In order to measure the catalytic activity of fumarate reductase under anaerobic conditions, 0–5 µ*M* purified Osm1 or trypsinized Osm1 was mixed with 100 m*M* fumarate (Sigma) and 50 µ*M* FAD (Sigma) in phosphate-buffered saline (PBS) with 1 m*M* EDTA. The FAD was reduced and anaerobic conditions were generated by adding sodium dithionite (Sigma) to a final concentration of 0.5%(*w*/*v*) and then sealing the plates to prevent exposure to oxygen. Once Osm1 had reduced the fumarate to succinate under anaerobic conditions, free flavin was oxidized by transferring electrons to

Osm1. The reoxidation of FAD by Osm1 was monitored by UV spectroscopy (BioTek), following the absorbance at 450 nm (oxidized FAD).

### 2.5. Crystallization

For crystallization, trypsin-resistant Osm1 was incubated with 500 µ*M* FAD, 10 m*M* maleic acid or 10 m*M* fumarate for 1 h on ice. Crystallization conditions were screened at 293 K by the two-drop sitting-drop vapour-diffusion method using screening kits from Hampton Research (Crystal Screen, Crystal Screen 2, Index, PEGRx, PEG/Ion and SaltRx). Crystals were grown on the plates by equilibrating a mixture comprising 200 nl protein solution and 200 nl reservoir solution against 0.1 ml reservoir solution. Optimized crystals were produced in reservoir solution consisting of 25%(*w*/*v*) PEG 3500, 0.2 *M* NaCl, 0.1 *M* bis-Tris pH 5.5 and were suitable for the collection of a data set. The crystals diffracted to 1.75 Å resolution. A summary of the crystallization conditions is provided in Table 2.

### 2.6. Data collection and processing

For data collection, crystals were transiently soaked in a solution corresponding to reservoir solution supplemented with 16%(*v*/*v*) glycerol. The soaked crystals were then flash-cooled in liquid nitrogen. Native diffraction data sets were collected on beamline 5C SBII at Pohang Accelerator Laboratory (PAL), Republic of Korea. A total of 360 images were collected with 1° oscillations. The data set was indexed and processed using *HKL*-2000 (Otwinowski & Minor, 1997). Diffraction data statistics are given in Table 3.

## 3. Results and discussion

Osm1 has a signal sequence at its N-terminus that directs it to the ER (Fig. 1). Since the signal sequence is highly hydrophobic, the N-terminal 32 amino acids including the signal sequence were deleted for the expression of Osm1 in the cytosol of *E. coli*. Instead, the Osm1 sequence (Met33–Tyr501) was fused to a 6×His tag and a thrombin-recognition sequence that originated from the pET-28a vector. Overexpressed Osm1

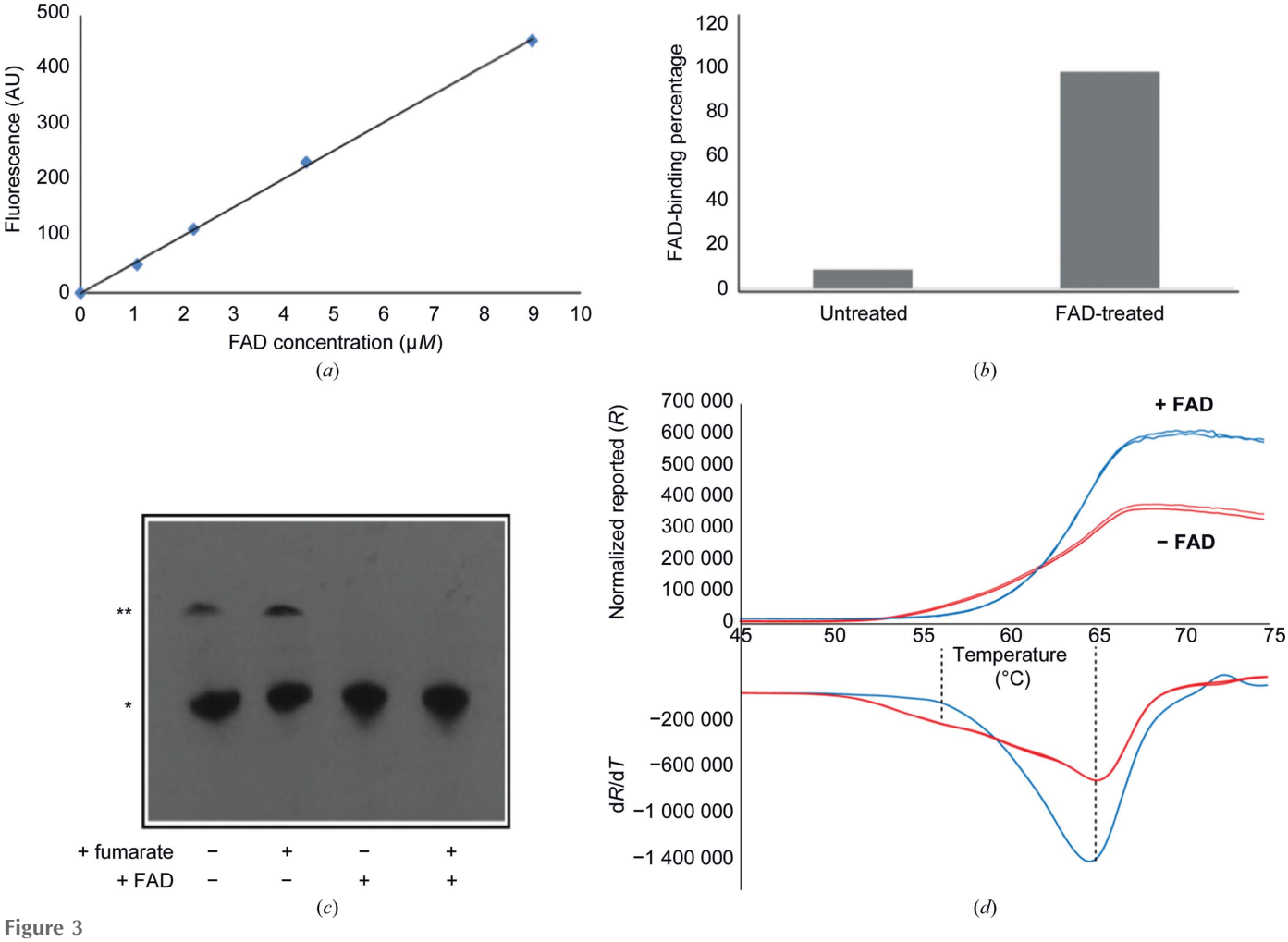


**Figure 3**
FAD cofactor binding to Osm1. (*a*) FAD standard curve based on fluorescence. The fluorescence of free FAD at different concentrations was measured using excitation at 450 nm and emission at 535 nm. (*b*) FAD cofactor-binding percentage of recombinant Osm1. FAD-binding percentages of recombinant Osm1 and FAD-treated recombinant Osm1 were calculated based on the protein concentration and bound FAD concentration. (*c*) The mobility of Osm1 with or without FAD cofactor and fumarate was compared on a native gel. (*d*) Changes in the thermal stability of Osm1 depending on FAD binding. Red lines indicate purified recombinant Osm1 and blue lines indicate recombinant Osm1 incubated with exogenous FAD.

was primarily found in the soluble fraction of the cell lysates and could easily be purified using an NTA column (Fig. 2*a*), indicating that the expressed Osm1 was well folded in the cytosol of *E. coli*. The Osm1 eluted from the NTA column was further purified by size-exclusion chromatography, which resulted in greater than 95% purity based on SDS–PAGE analysis (Fig. 2*b*).

Purified Osm1 showed a marginal yellow colour, which must be caused by the FAD cofactor. To calculate the percentage of FAD binding in recombinant Osm1 expressed in bacteria, the protein and FAD concentrations were calculated by the Bradford assay and by the measurement of FAD fluorescence, respectively. The amount of protein was then calculated based on comparison with a BSA standard curve. Since the fluorescence of free FAD could differ from that of protein-bound FAD (Nakashima *et al.*, 1980), FAD cofactor was separated from Osm1 by denaturing Osm1 in 6 *M* guanidine–HCl. The Osm1-bound FAD concentration was calculated by comparison with a standard FAD fluorescence curve generated with excitation and emission at 450 and 535 nm, respectively (Fig. 3*a*). Recombinant Osm1 expressed in bacteria showed less than 10% FAD binding, suggesting that Osm1 can be stably folded even in the absence of the FAD cofactor. To generate fully holo Osm1, recombinant Osm1 was incubated with a molar excess of FAD, after which unbound FAD was removed. FAD-treated Osm1 showed greater than 90% FAD-binding efficiency, indicating that the FAD cofactor can efficiently incorporate into apo Osm1 exhibiting correct folding. The FAD deficiency of recombinant Osm1 may be caused by low levels of free FAD in the expression bacteria. In support of this suggestion, supplementation of the LB medium with FAD increased the FAD-binding level in overexpressed Osm1.

The biophysical properties of apo Osm1 and holo Osm1 were compared in this study. Interestingly, native gel electrophoresis showed that some fraction of recombinant Osm1 migrated like an oligomer, but that this disappeared upon the addition of FAD (Fig. 3*c*). These results indicated that purified recombinant Osm1 was not homogenous because the fractions of apo Osm1 and FAD-bound Osm1 might be in different oligomeric states. However, fumarate, a natural substrate of Osm1, did not affect the oligomeric state of apo Osm1. We next measured the thermal stability upon FAD binding using a thermal shift assay. Interestingly, apo Osm1 started to denature at lower temperatures (two transition temperatures at 57 and 65°C) than holo Osm1 (one major transition temperature at 65°C), indicating that apo Osm1 was less stable than holo Osm1 (Fig. 3*d*). Based on these results, we decided to purify and crystallize recombinant Osm1 after incubating it with FAD to stabilize the Osm1 and increase its homogeneity by minimizing the percentage of apo Osm1.

Initial crystal screening with holo Osm1 and fumarate or maleic acid showed that only needle-like isotropic crystals formed in 0.1 *M* Tris pH 8.5, 0.2 *M* $LiSO_4$, 30% PEG 4000 or 30% mPEG 5000 (Figs. 4*a* and 4*b*). However, these crystals were not of sufficient quality for structural analysis. Prior to optimizing the crystallization conditions, we attempted to remove all flexible fragments from Osm1 by using limited proteolysis. Recombinant Osm1 was treated with a small amount of trypsin for a limited time on ice to obtain the

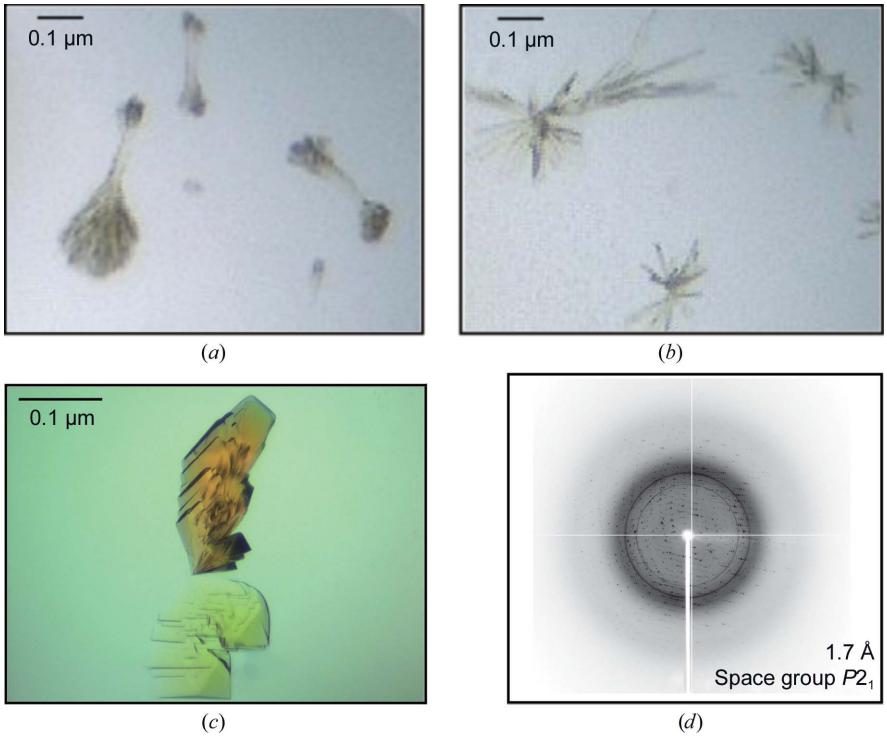


**Figure 4**
Crystallization and X-ray diffraction. (*a*) Intact recombinant Osm1 crystals formed in 30% PEG 4000, 0.1 *M* Tris pH 8.5, 0.2 *M* $LiSO_4$ and (*b*) in 30% mPEG 5000, 0.1 *M* Tris pH 8.0, 0.2 *M* $LiSO_4$. (*c*) Trypsin-resistant Osm1 crystals formed in 0.2 *M* NaCl, 0.1 *M* bis-Tris pH 5.5, 25% PEG 3500. (*d*) The crystals in (*c*) showed single-crystal diffraction to around 1.75 Å resolution and belonged to space group $P2_1$.

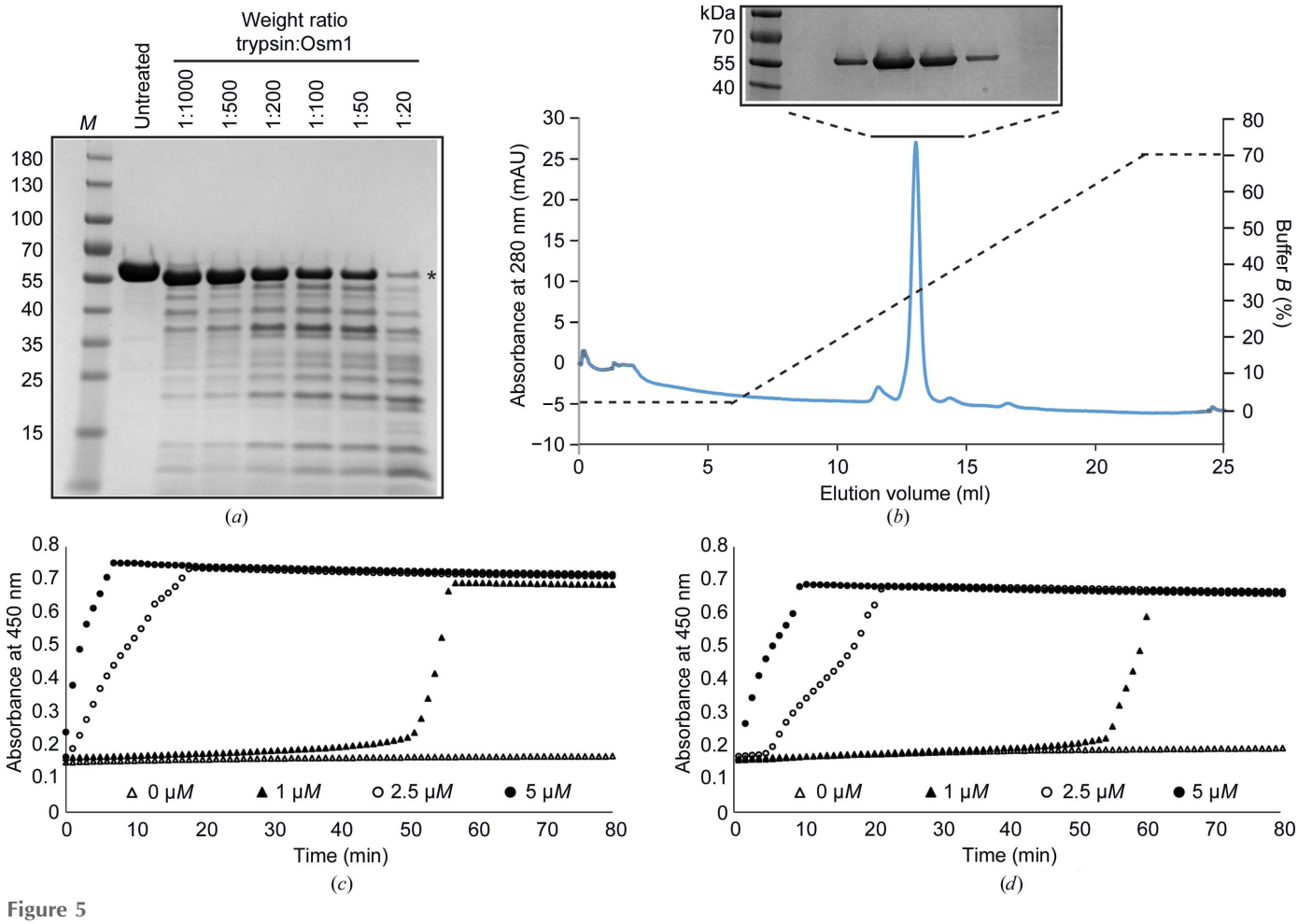


**Figure 5**
Limited proteolysis of Osm1. (*a*) Osm1 was treated with trypsin and analyzed by SDS–PAGE. The asterisk indicates the dominant trypsin-resistant Osm1 fragment. Lane *M*, molecular-mass markers (labelled in kDa). (*b*) Cation-exchange chromatogram for the purification of the trypsin-resistant Osm1 fragment. The sample was eluted with a salt gradient. Fractions corresponding to the major peaks were analyzed by SDS–PAGE and are shown in the inset. (*c*, *d*) Catalytic activity of Osm1. 6×His-tagged Osm1 (*c*) or trypsinized Osm1 (*d*) was mixed with 100 m*M* fumarate and 50 µ*M* FAD. The oxidation of FAD by fumarate reductase was monitored by the absorbance at 450 nm ($A_{450}$) after reducing the FAD and mimicking anaerobic conditions by adding sodium dithionite.

trypsin-resistant fragment. Interestingly, limited proteolysis of Osm1 showed a dominant trypsin-resistant band at 55 kDa, which migrated slightly faster than intact recombinant Osm1 (∼60 kDa; Fig. 5*a*). Trypsin-resistant Osm1 showed very weak binding to NTA beads (data not shown), indicating that the N-terminal flexible region (∼5 kDa), including the 6×His tag, might be removed by limited proteolysis. At a 1:500 weight ratio of trypsin:Osm1, intact recombinant Osm1 disappeared almost completely, but the amount of trypsin-resistant Osm1 was maximized. The trypsin-resistant Osm1 was further purified by ion-exchange chromatography, which removed most of the impurities (Fig. 5*b*). We measured the fumarate reductase activity of intact Osm1 and trypsinized Osm1 after mimicking anaerobic conditions and reducing FAD using sodium dithionite. The removal of a flexible fragment from intact Osm1 did not affect its catalytic activity (Figs. 5*c* and 5*d*), indicating that trypsinized Osm1 maintains an active conformation.

Crystals of trypsin-resistant Osm1 in the presence of FAD and fumarate were grown in 0.2 *M* sodium chloride, 0.1 *M* bis-Tris pH 5.5, 25% polyethylene glycol 3350 (Fig. 4*c*). These crystals were dark yellow, indicating that holo Osm1 containing FAD cofactors was present in the crystals. These crystals also diffracted to 1.75 Å resolution (Fig. 4*d*), which was sufficient to solve the precise structure of Osm1. The soluble protein and diffracting crystals of Osm1 were successfully obtained by biochemical and limited proteolytic assays. The crystals were found to belong to space group $P2_1$. Assuming the presence of one molecule in the crystallographic asymmetric unit, the Matthews coefficient ($V_M$) was calculated to be 2.72 Å$^3$ Da$^{-1}$, which corresponds to a solvent content of 54.71% (Matthews, 1968). The diffraction data statistics are given in Table 3. The data set was indexed and processed using *HKL*-3000 (Minor *et al.*, 2006).

## Funding information

This study was supported by Chung-Ang University Research Grants in 2018 and the Basic Science Research Program through the National Research Foundation of Korea (NRF) of

the Ministry of Education, Science and Technology (NRF-2014R1A1A1003451).

## References

Arikawa, Y., Enomoto, K., Muratsubaki, H. & Okazaki, M. (1998). *FEMS Microbiol. Lett.* **165**, 111–116.
Bamford, V., Dobbin, P. S., Richardson, D. J. & Hemmings, A. M. (1999). *Nature Struct. Biol.* **6**, 1104–1107.
Bergdahl, B., Gorwa-Grauslund, M. F. & van Niel, E. W. (2014). *BMC Biotechnol.* **14**, 28.
Cecchini, G., Schröder, I., Gunsalus, R. P. & Maklashina, E. (2002). *Biochim. Biophys. Acta*, **1553**, 140–157.
Enomoto, K., Arikawa, Y. & Muratsubaki, H. (2002). *FEMS Microbiol. Lett.* **215**, 103–108.
Liu, Z., Österlund, T., Hou, J., Petranovic, D. & Nielsen, J. (2013). *Appl. Environ. Microbiol.* **79**, 2962–2967.
Matthews, B. W. (1968). *J. Mol. Biol.* **33**, 491–497.
Minor, W., Cymborowski, M., Otwinowski, Z. & Chruszcz, M. (2006). *Acta Cryst.* D**62**, 859–866.
Miura, A., Kameya, M., Arai, H., Ishii, M. & Igarashi, Y. (2008). *J. Bacteriol.* **190**, 7170–7177.
Muratsubaki, H. & Enomoto, K. (1998). *Arch. Biochem. Biophys.* **352**, 175–181.
Nakashima, N., Yoshihara, K., Tanaka, F. & Yagi, K. (1980). *J. Biol. Chem.* **255**, 5261–5263.
Otwinowski, Z. & Minor, W. (1997). *Methods Enzymol.* **276**, 307–326.
Pealing, S. L., Black, A. C., Manson, F. D., Ward, F. B., Chapman, S. K. & Reid, G. A. (1992). *Biochemistry*, **31**, 12132–12140.
Reid, G. A., Miles, C. S., Moysey, R. K., Pankhurst, K. L. & Chapman, S. K. (2000). *Biochim. Biophys. Acta*, **1459**, 310–315.
Williams, C. C., Jan, C. H. & Weissman, J. S. (2014). *Science*, **346**, 748–751.
Zielinska, D. F., Gnad, F., Schropp, K., Wiśniewski, J. R. & Mann, M. (2012). *Mol. Cell*, **46**, 542–548.